

High-dynamic-range transmission-mode detection of synchrotron radiation using X-ray excited optical luminescence in diamond

Stanislav Stoupin,^{a*} Sergey Antipov^b and Alexander M. Zaitsev^{c,d}

Received 8 November 2019

Accepted 28 January 2020

Edited by A. Bergamaschi, Paul Scherrer Institut, Switzerland

Keywords: diamond; X-ray scintillator; NV defects; beam profile imaging.

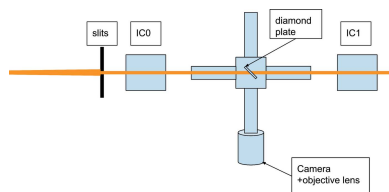
^aCornell High Energy Synchrotron Source, Cornell University, Ithaca, NY 14853, USA, ^bEuclid Techlabs LLC, Solon, OH 44139, USA, ^cCollege of Staten Island and Graduate School of the City University of New York, Staten Island, NY 10314, USA, and ^dGemological Institute of America, New York, NY 10036, USA.

*Correspondence e-mail: sstoupin@cornell.edu

Enhancement of X-ray excited optical luminescence in a 100 µm-thick diamond plate by introduction of defect states via electron beam irradiation and subsequent high-temperature annealing is demonstrated. The resulting X-ray transmission-mode scintillator features a linear response to incident photon flux in the range 7.6×10^8 to 1.26×10^{12} photons $\text{s}^{-1} \text{mm}^{-2}$ for hard X-rays (15.9 keV) using exposure times from 0.01 to 5 s. These characteristics enable a real-time transmission-mode imaging of X-ray photon flux density without disruption of X-ray instrument operation.

1. Introduction

Noninvasive (or minimally invasive) visualization of X-ray beam profiles under *in operando* conditions is of high practical importance at experimental stations of large-scale synchrotron and XFEL user facilities. The desired generalized device functionality can be described as real-time imaging of flux density distribution in a chosen observation plane placed across the direction of propagation of the X-ray beams. Common metrics, which reflect the performance of the experimental station, such as average beam position, intensity/photon flux over a chosen region of interest as well as position and intensity fluctuations, can be derived from the real-time profiles of flux density. A recently demonstrated, quantitative approach for flux density monitoring features detection of electrical charge in a lithographically patterned (pixelated) diamond plate (Zhou *et al.*, 2015). X-ray transmission-mode scintillators (producing X-ray excited optical luminescence) with low X-ray absorption, coupled to visible-light area detectors, is an alternative, more straightforward strategy towards the implementation of the imaging functionality. Diamond is a preferable choice for the X-ray transmission-mode scintillator due to its low X-ray absorption, high radiation hardness, and remarkable thermal and mechanical properties. Video monitoring of X-ray excited optical luminescence in thin diamond plates is commonly used for this purpose, however, predominantly in a semi-quantitative manner, where the observed profile is evaluated based on visual appearance characteristics (*e.g.* spatial resolution, relative brightness) often without documented knowledge on response linearity and dynamic detection range. Such advanced characterization is perhaps unnecessary for monitoring profiles of intense synchrotron beams upstream of the beamline monochromator (beamline front-end) (Degenhardt *et al.*, 2013; Kosciuk *et al.*, 2016; Takahashi *et al.*, 2016). In



© 2020 International Union of Crystallography

other cases (e.g. X-ray beams downstream of the monochromator), a more quantitative approach is required. Park *et al.* (2018) recently demonstrated $\sim 3 \mu\text{m}$ beam position stability for a monochromatic beam using a commercial diamond screen as a real-time imaging detector. However, no information on the response linearity is provided, and therefore the dynamic detection range of their study remains unclear. In this work, we achieved enhancement of X-ray optical luminescence in a thin diamond plate by introduction of additional defects via electron irradiation and subsequent high-temperature annealing. The resulting responsivity and the dynamic range of the luminescence detection were increased by more than one order of magnitude compared with commercially available diamond screens of the same thickness. Contrary to the commercial diamond screens, the response to the incident X-ray photon flux was found to be linear in the range 7.6×10^8 to 1.26×10^{12} photons $\text{s}^{-1} \text{mm}^{-2}$.

2. Samples

The samples procured for this study were circular polycrystalline diamond plates prepared using chemical vapor deposition (CVD) with diameter of 10 mm and thickness of 100 μm . These were of the nominal ‘tool’, ‘thermal’ and ‘optical’ grades (supplier specification), presumably of different impurity concentration. An additional polycrystalline diamond plate of the ‘optical’ grade of the same shape was acquired from the same supplier. It was subjected to irradiation and subsequent annealing to generate luminescent centers (irradiated and annealed plate). To create vacancies in the diamond lattice, irradiation was performed with an energetic electron beam. Practically any diamond contains impurities. Both diamond plates of the ‘optical’ grade had a completely transparent visual appearance. The main impurity was N with expected concentration on the order of 0.1–10 parts per million (p.p.m.). Annealing was performed in vacuum to promote formation of nitrogen vacancy (NV) defect centers. In this work we made no attempts to study boron-doped diamond samples for the following reasons. While it is known that some natural and synthetic boron-doped single crystals produce enhanced luminescence, the characteristic luminescence lifetimes are on the order of seconds (Eaton-Magaña & Lu, 2011; Gaillou *et al.*, 2012), which can result in a nonlinear response for real-time detection. Prior studies indicate that boron is not an efficient luminescent center in boron-doped polycrystalline CVD diamond (Graham *et al.*, 1994; Iakoubovskii & Adriaenssens, 2000a).

Luminescence spectra under UV excitation at a wavelength of 360 nm were measured for all samples. Selected spectra are shown in Fig. 1. The luminescence spectrum of the unannealed ‘optical’ grade sample (hereon referred to as ‘optical’) is shown by a yellow dashed line. It can be described as a broad band with a maximum response in the spectral range from 500 to 600 nm. This band is due to characteristic optically active defects, which usually dominate luminescence of as-grown nitrogen-doped CVD diamonds. In luminescence measured at

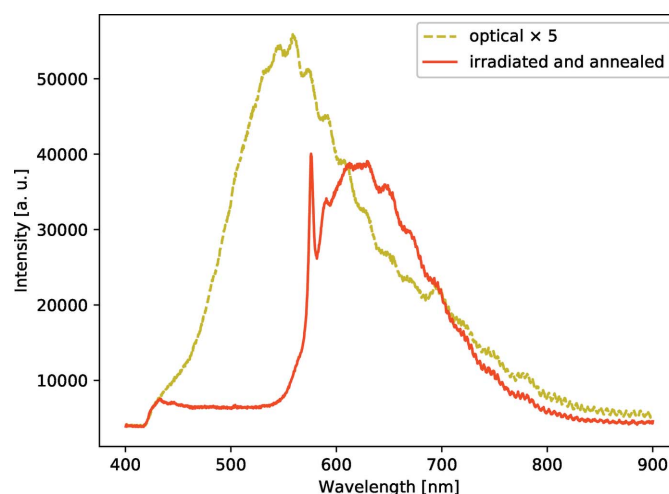


Figure 1 Spectra of UV-excited luminescence in the irradiated and annealed diamond plate (red solid line) and diamond plate of optical grade (yellow dashed line; data collected using five times longer exposure time per point).

low temperature, these optical centers produce a zero-phonon line at wavelength of 468 nm (not clearly seen in the present spectrum recorded at room temperature) (Zaitsev, 2001; Iakoubovskii & Adriaenssens, 2000b). Although the 486 nm center is very typical for nitrogen-doped CVD diamonds, its origin has not been identified yet. The luminescence spectrum of the ‘thermal’ grade sample was found to be relatively weak, having similar spectral shape (not shown in the figure). The sample of ‘tool’ grade did not produce any reasonably measurable luminescence. The spectral response of the irradiated and annealed sample (shown by a red solid line) was much stronger compared with that of the ‘optical’ grade sample. Its appearance is characteristic of the NV0 center (Zaitsev, 2001), which includes the zero-phonon line (narrow peak at 575 nm) and the broad phonon side-band above it.

3. Experiment, results and discussion

The characterization experiment was conducted at 2B beam-line of Cornell High Energy Synchrotron Radiation Source (CHESS, Cornell University, USA). The beamline features CHESS compact undulator (Temnykh *et al.*, 2013) and a side-bounce diamond monochromator (Stoupin *et al.*, 2019a,b) operating at a set of fixed photon energies (9.7, 15.9, 18.65, 22.5 keV). Diamond screens were placed in a light-tight environment at 45° with respect to the incident X-ray beam, which was shaped to 1 mm \times 1 mm size using X-ray slits. X-ray excited luminescence was measured using a Mako G319C camera (Allied Vision) equipped with an objective lens. The camera was placed at a distance of about 100 mm from the sample. An ionization chamber (IC0) was placed upstream of the diamond screen to monitor the incident photon flux, and another ionization chamber (IC1) was set downstream of the diamond to monitor photon flux transmitted through the sample. The experimental setup is shown schematically in Fig. 2 (top view).

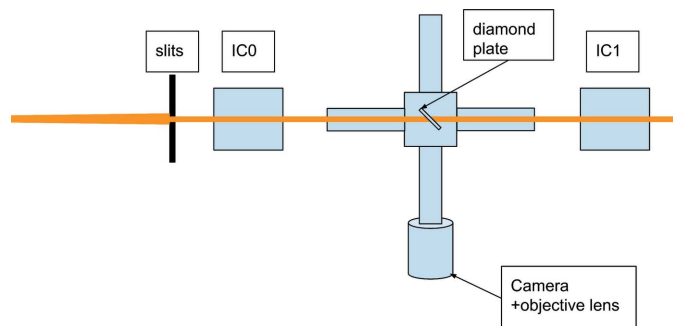


Figure 2
Experimental setup (top view); see text for details.

During preliminary tests with the X-ray beam, the luminescence intensity of the ‘tool’ grade sample was found to be negligible compared with that of other samples. Therefore, results for this sample were excluded from the analysis. This can be easily explained by the dark appearance of the sample (high self-absorption of luminescence). The X-ray transmissivity was measured at 15.9 keV. The observed values were 0.965, 0.969 and 0.973 for the thermal, optical and the irradiated plates, respectively. For a 100 μm -thick diamond plate oriented at 45° with respect to the incident beam the transmission factors calculated using tabulated values for the mass attenuation coefficient and the mass energy-absorption coefficient (Hubbell & Seltzer, 2004) are 0.965 and 0.977, respectively. Thus, X-ray attenuation in the diamond plates was small, as expected. In the first experiment, the linearity of the system was explored by performing measurements at a fixed incident photon flux at 15.9 keV using different exposure times. The range of exposure times was from 0.01 up to 5 s (except for a few 10 s exposures for the weakly luminescent ‘thermal’ grade sample). This range could be described as real-time conditions for most experiments performed at synchrotron sources (excluding fast time-resolved experiments). The response was measured as a sum of pixel intensity across the image of the beam footprint, normalized by the number of pixels. An offset representing camera dark current (sum of pixel intensity for a region of the same size, not exposed to X-rays) was subtracted. The fluctuation of the response was found to be less than 1%. In the figures that follow, the related uncertainties are less than the size of the figure markers. The values of the photon flux were evaluated using an ion chamber flux calculator for an N_2 -filled chambers of length 6 cm (Revesz, 2007). The response as a function of exposure time was found to be linear to within experimental uncertainties for all studied diamond plates. The results are shown in Fig. 3.

This observation enabled further characterization of the luminescence as a function of the incident photon flux regardless of exposure time (normalization of the response by the exposure time was performed). Since the dynamic range of the camera was only 12 bit (up to 4096 counts per pixel), variable exposure time enabled greater total dynamic range for quantitative evaluation of luminescence intensity. In the second experiment the luminescence was evaluated at variable incident flux levels at a photon energy of 15.9 keV. The time-normalized response (response hereon) as a function of the

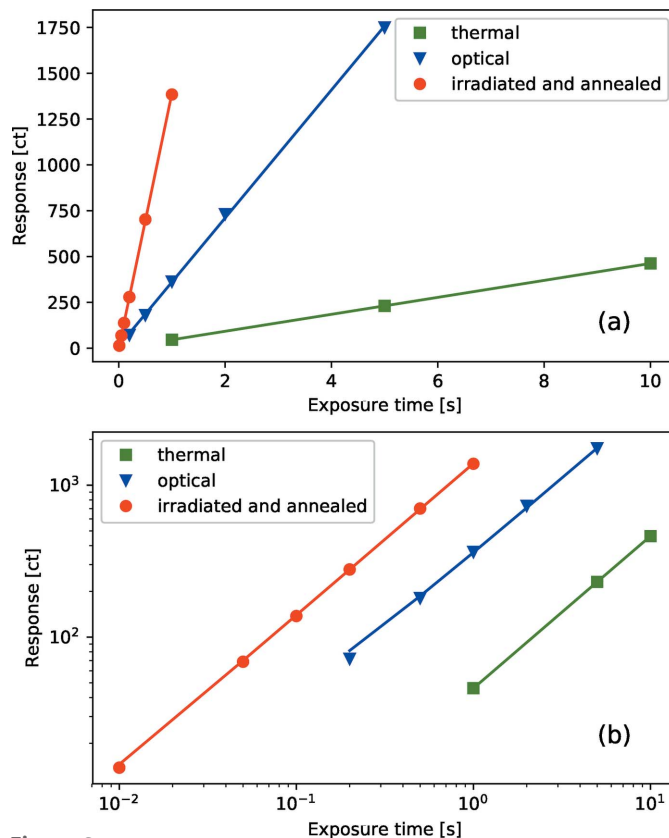


Figure 3
X-ray excited optical luminescence (average response over the 1 mm \times 1 mm X-ray beam footprint) as a function of exposure time for the as-received diamond plates (thermal and optical grades) and for the irradiated and annealed plate. The linear–linear plot (a) is supplemented with a log–log plot (b). The solid lines are fits to the linear function.

incident photon flux for the different diamond plates is shown in Fig. 4. Fits with a linear function are shown by the solid lines. The proportionality coefficients in the linear fits were 3.7×10^{-11} , 2.9×10^{-10} , and 3.2×10^{-9} for the thermal, optical, and irradiated and annealed samples, respectively. For the sample of thermal grade, only two data points were measured, which precludes analysis of response linearity. The response of the optical grade sample deviates from the linear behavior (as shown by the dashed line), which reduces the dynamic range for detection of photon flux, while the response of the irradiated and annealed sample is linear to a good approximation. The response of the irradiated sample is greater by more than one order of magnitude. The resulting measured dynamic detection range is more than three orders of magnitude. The detected levels of the photon flux are from 7.6×10^8 to 1.26×10^{12} photons s^{-1} .

Fig. 5 shows color images (RGB) of the X-ray beam footprint taken at 15.9 keV. Different exposure times and flux levels were used to optimize image statistics.

For the samples of thermal and optical grades the luminescence color is predominantly in the blue range. We note that the luminescence spectrum measured under UV excitation (Fig. 1) corresponds to green color. This discrepancy suggests non-equivalence of X-ray and UV excitation. A more detailed interpretation of this observation falls outside the

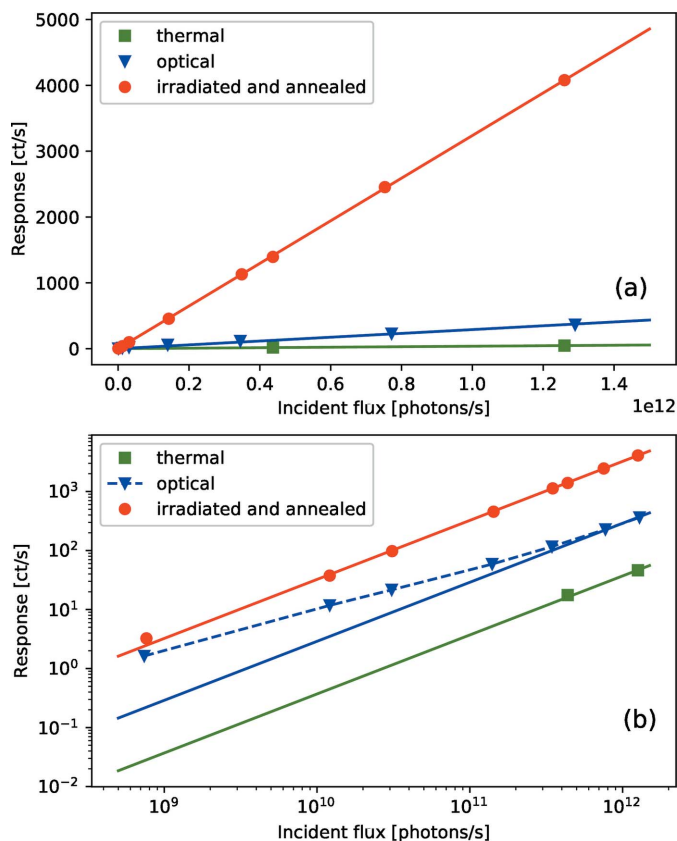


Figure 4 X-ray excited optical luminescence (average time-normalized response over the 1 mm × 1 mm X-ray beam footprint) as a function of the incident photon flux for the as-received diamond plates (thermal and optical grades) and for the irradiated and annealed plate. The linear-linear plot (a) is supplemented with a log-log plot (b). The dashed line connecting data for the optical grade sample in (b) illustrates nonlinear behavior. The solid lines are fits to the linear function.

scope of the present study. For the irradiated and annealed sample the luminescence color is predominantly red due to the characteristic NV0 luminescence (consistent with the UV-excited luminescence spectrum). Some structure in luminescence of the irradiated sample was observed (lines of intensity propagating outside of the X-ray illuminated region). We attribute this effect to surface quality (luminescence re-scattering on surface defects/scratches).

In the final experiment the response of the irradiated and annealed sample was measured at the several fixed photon energies available at the beamline. Under the conditions of negligible re-scattering and self-absorption of luminescence,

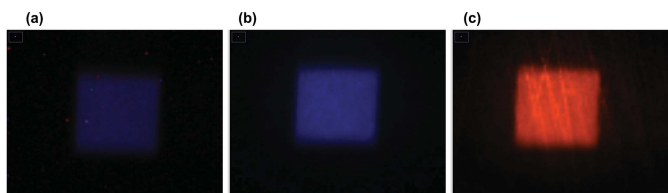


Figure 5 Color images of X-ray excited optical luminescence in diamond plates of different grades: thermal (a), optical (b), irradiated and annealed sample (c).

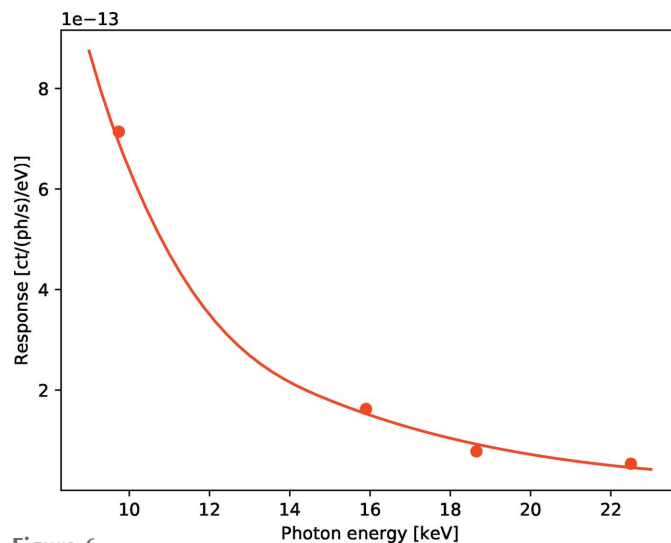


Figure 6 X-ray excited optical luminescence (average energy-normalized response over the 1 mm × 1 mm X-ray beam footprint) as a function of the X-ray photon energy for the irradiated and annealed diamond plate. The solid line represents the scaled absorptivity of X-rays in the 100 μm-thick diamond plate [equation (1)].

which are applicable to the thin diamond plate of the optical grade, the response as a function of the X-ray photon energy E_X can be approximated by (Rogalev & Goulon, 2002)

$$R(E_X) \propto F_0 E_X \{1 - \exp[-\mu(E_X)t]\}, \quad (1)$$

where F_0 is the incident photon flux, $\mu(E_X)$ is the X-ray attenuation coefficient of the material (for practical purposes the mass-energy attenuation coefficient is often used), and t is the thickness of the plate. Here it is assumed that the energy conversion efficiency and the quantum yield do not depend on the X-ray photon energy, which is a valid assumption for hard X-rays since the photon energies are substantially above the characteristic energies of any electronic transitions of the carbon atom. Fig. 6 shows the measured luminescence response normalized by F_0 and E_X as a function of the photon energy. This ratio should be proportional to the absorptivity of the diamond plate according to equation (1). The absorptivity of the sample for a 100 μm-thick plate, scaled to the experimental data using the optimal proportionality coefficient, is plotted with a solid line. The agreement between the experiment and equation (1) is good. The observed minor discrepancies can be attributed to uncertainties in determination of the incident photon flux.

4. Summary

In summary, we have demonstrated a more than one order of magnitude improvement in responsivity of X-ray excited luminescence in a thin (nearly transparent for hard X-rays) diamond scintillator by introduction of NV defect states. The results of synchrotron X-ray measurements show that the new scintillator has a linear response to the incident hard X-ray flux density in the range from 7.6×10^8 to 1.26×10^{12} photons $s^{-1} mm^{-2}$. This was demonstrated using a simple imaging

scheme in the visible range with exposure times for individual frames from 0.01 to 5 s. Thus, an imaging device using the new scintillator can provide minimally invasive real-time transmission-mode imaging of photon flux density without disruption of X-ray instrument operation. Further improvement in responsivity can be achieved by exploring other highly luminescent defect centers, reducing the influence of competing non-radiative processes (*e.g.* via control of crystal lattice quality) (Antipov *et al.*, 2019) as well as by using more advanced imaging detectors and image intensifiers. Future work could be extended to detailed studies of spatial resolution and time response of the new scintillator. Outcomes of such studies may lead to the next-generation technology for beam diagnostics at large-scale X-ray user facilities.

Acknowledgements

This work is based upon research conducted at the Cornell High Energy Synchrotron Source (CHESS) which is supported by the National Science Foundation (see funding details below).

Funding information

Funding for this research was provided by: NSF (award No. DMR-1332208); DOE SBIR (award No. DE-SC0019628).

References

Antipov, S., Stoupin, S. & Zaitsev, A. (2019). US Patent application 16/659642.

- Degenhardt, M., Aprigliano, G., Schulte-Schrepping, H., Hahn, U., Grabosch, H.-J. & Wörner, E. (2013). *J. Phys. C*, **425**, 192022.
- Eaton-Magaña, S. & Lu, R. (2011). *Diamond Relat. Mater.* **20**, 983–989.
- Gaillou, E., Post, J. E., Rost, D. & Butler, J. E. (2012). *Am. Mineral.* **97**, 1–18.
- Graham, R. J., Shaapur, F., Kato, Y. & Stoner, B. R. (1994). *Appl. Phys. Lett.* **65**, 292–294.
- Hubbell, J. & Seltzer, S. (2004). *NIST Standard Reference Database 126*, <https://physics.nist.gov/PhysRefData/XrayMassCoef/tab3.html>.
- Iakoubovskii, K. & Adriaenssens, G. J. (2000a). *Phys. Rev. B*, **61**, 10174–10182.
- Iakoubovskii, K. & Adriaenssens, G. (2000b). *Phys. Status Solidi A*, **181**, 59–64.
- Kosciuk, B., Hu, Y., Keister, J. & Seletskiy, S. (2016). *AIP Conf. Proc.* **1741**, 020030.
- Park, J. Y., Kim, Y., Lee, S. & Lim, J. (2018). *J. Synchrotron Rad.* **25**, 869–873.
- Revesz, P. (2007). *Ion Chamber Flux Calculator*, <https://www.chess.cornell.edu/users/calculators/ion-chamber-flux-calculator>.
- Rogalev, A. & Goulon, J. (2002). In *Chemical Applications of Synchrotron Radiation*, edited by T.-K. Sham. New Jersey, London, Singapore, Hong Kong: World Scientific.
- Stoupin, S., Krawczyk, T., Liu, Z. & Franck, C. (2019a). *Crystals*, **9**, 396.
- Stoupin, S., Krawczyk, T., Ruff, J. P. C., Finkelstein, K. D., Lee, H. H. & Huang, R. (2019b). *AIP Conf. Proc.* **2054**, 060019.
- Takahashi, S., Kudo, T., Sano, M., Watanabe, A. & Tajiri, H. (2016). *Rev. Sci. Instrum.* **87**, 083111.
- Temnykh, A., Dale, D., Fontes, E., Li, Y., Lyndaker, A., Revesz, P., Rice, D. & Woll, A. (2013). *J. Phys. Conf. Ser.* **425**, 032004.
- Zaitsev, A. M. (2001). *Optical Properties of Diamond: A Data Handbook*. Berlin: Springer.
- Zhou, T., Ding, W., Gaowei, M., De Geronimo, G., Bohon, J., Smedley, J. & Muller, E. (2015). *J. Synchrotron Rad.* **22**, 1396–1402.